Pure appl. geophys. 165 (2008) 475–496
0033–4553/08/030475–22
DOI 10.1007/s00024-008-0324-x



Pure and Applied Geophysics

# Modeling and Visualization of Tsunamis

HUAI ZHANG,[1] YAOLIN SHI,[1] DAVID A. YUEN,[1,2] ZHENZHEN YAN,[1] XIAORU YUAN,[3] and CHAOFAN ZHANG[1]

*Abstract*—Modeling tsunami wave propagation is a very challenging numerical task, because it involves many facets: Such as the formation of various types of waves and the impingement of these waves on the coast. We will discuss the different levels of approximations made in numerical modeling of 2-D and 3-D tsunami waves and their relative difficulties. In this paper new attempts are proposed to evaluate the hazards of tsunami's and visualization of large-scale numerical results generated from tsunami simulations. Specialized low-level computer language, based on a parallel computing environment, is also employed here for generating FORTRAN source code for finite elements. This code can then be run very efficiently in parallel on distributed computing systems. We will also discuss the need to study tsunami waves with modern software and visualization hardware.

**Key words:** Tsunami, wave propagation, parallel simulation environment, visualization.

## 1. Introduction

Following the great Sumatran earthquake on December 26, 2004, the Indian Ocean tsunami and the accompanying tsunami waves caused widespread damage and killed more than 225,000 people within a few hours and left millions of people homeless. This event has indeed awakened great scientific interest in tsunami wave propagation over undulated seafloor topography, and along irregular coastlines. Traditional analytical approximations are valid over long wavelengths in the far field. This can be used as a first measure for tsunami prediction and warning (http://tsunami.jrc.it/model/model.asp). But for near-field regions with complex geography and other complications, such as islands and harbors, "high resolution" numerical simulation must be employed to obtain accurate predictions in both space and time. Presently using 10 million to 100 million grid points becomes commonplace with improved dual-core laptops and also massively parallel computers with access to huge data and high-speed I/O support. Besides tsunamis,

[1] Laboratory of Computational Geodynamics, Graduate University of Chinese Academy of Sciences, Beijing 100049, China. E-mail: hzhang@gucas.ac.cn

[2] Department of Geology and Geophysics, University of Minnesota, Minneapolis, MN 55455, U.S.A.

[3] State Key Laboratory of Machine Perception, and Dept. of Machine Intelligence, School of EECS, Peking University, Beijing 100871, China.

turbulent river discharges from upstream events and tall waves driven by hurricanes or by huge tankers, will also cause severe damage to dams and the foundation of mountain slopes. This aspect is of societal relevance, especially the Three Gorges project in central China along the Yangtze River.

Although the frequency of earthquake-generated tsunamis around the globe is relatively low compared to many other natural hazards, such as earthquakes, volcanoes, and hurricanes, the terrible Sumatran tsunami event was still an unforgettable reminder that the damaging impacts of tsunamis may remain extremely high in human history. Especially, with the booming of the population along coastal regions in recent years around the world, this type of shocking disaster will pose even greater risk than ever before (TIBBETTS, 2002). Tsunami propagation is thus a problem with global dimensions, knowing no international boundaries across the sea. There is currently a great need for understanding better tsunami wave propagation, which calls for comparison of simulations with detailed data from observations. Fortunately, fast developments of geographical information systems (GIS), the global positioning system (GPS), remote sensing techniques, such as Interferometric Synthetic Aperture Radar (InSAR) (CHANG, *et al*., 2005; NAEIJE, *et al*., 2002) and other modern observational technologies, enable scientists in the research fields of tsunami sciences to obtain daily huge amounts of data. These data, together with numerical results, can help researchers to better understand this deadly natural disaster. The Sumatran tsunami was without doubt the best documented case in history (TITOV *et al*., 2005). From videos of the run-up processes to direct satellite observations of the waves propagating in the far field, research scientists now have an unprecedented opportunity to study these catastrophes (http://www.asiantsunamivideos.com/). One important task facing the earth science community is to develop reliable easy-to-use software tools for facile modeling and visualization of tsunamis.

The objective of tsunami modeling research is now focused on developing numerical models for more accelerated and more reliable forecasting of tsunamis propagating through vast oceans before they strike the coastlines (MEINIG *et al*., 2005; TITOV and Gonzalez 1997, TITOV *et al*., 1999; GONZALEZ *et al*., 1995; MOFJELD *et al*., 2000). Some models can easily be satisfied by two-dimensional shallow water equations, while other models use slightly modified Navier-Stokes equations, which can enable the researcher to proceed beyond just the first-order physical phenomena (GILL 1982; PEDLOSKY 1987). We simply arrange these models in Figure 1.

Due to the alteration of ray patterns over complex bathymetry, tsunamis can be significantly modified while they are propagating over transoceanic areas, leading to the alteration of wave fronts and wave groups, frequently dispersion effects, and changes in spatial distribution of wave energy. Under such circumstances, Boussinesq approximation and Boussinesq equations are well known for their descriptions of such phenomena (KENNEDY and KIRBY, 2003). Boussinesq equations are obtained from the Euler equations with rotation, which include the effects of weak dispersion and nonlinearity in a shallow water framework and allow accurate near-shore simulation of wave transformation processes. Up to date, the extended Boussinesq equation systems allow the models to be

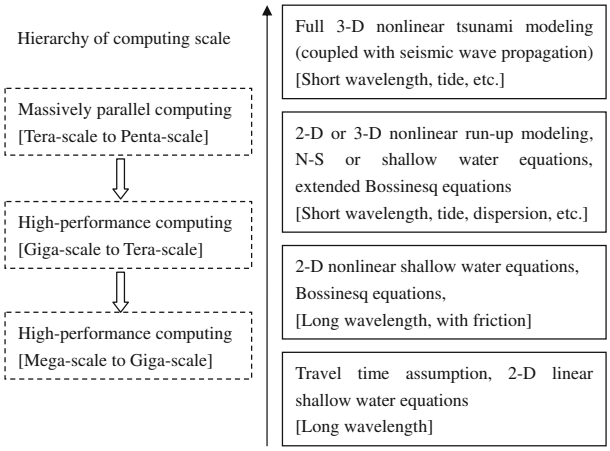


Figure 1
Hierarchy of tsunami models and computing scales.

applied in deeper water over relatively narrow and complex bathymetry so as to extend the range of applications, as well as increasing the accuracy of the linear dispersion characteristics of these models (WALKLEY and BERZINS, 2002). Parameters can be introduced to characterize horizontal wave packet length scale and aspect ratio which can describe dispersion effects. Those extended Boussinesq equations would be more appropriate to local wave evolution both near the tsunami source and in the final run-up stage. Those effects include representation of bottom motion, sea-bed friction and fully nonlinear treatment of surface conditions in order to represent large run-up amplitudes during inundation which can all be modeled and simulated by extended Boussinesq equation systems via retaining several aspects of parameterized formulations (KIRBY and DALRYMPLE, 1986; KENNEDY *et al*., 2000; CHEN *et al*., 2000).

There are several computational issues worthy of consideration. They deal with wave propagation over both short distances (near field) and long distances (far field). To date, most tsunami simulations have been carried out in two dimensions with the latitude and longitude being the independent variables. Three-dimensional simulations of tsunami waves including run-up, remain a grand-challenge problem because of the multiple-scale nature of the phenomenon (GICA and TENG, 2003; TITOV *et al*., 2005). Three-dimensional equations cannot be employed to solve real-time problems, due to the still inordinately long computational time.

Two-dimensional equations are more commonly used and can be used in places where warning must be issued in a timely fashion (TANG *et al*., 2006; GEIST *et al*., 2006; SMITH *et al*., 2005). Within the framework of two-dimensional tsunami equations, there are linear and nonlinear approximations with the linear shallow-water equations being the most popularly employed, since they are the simplest to implement and provide reliable answers regarding the travel time of tsunami waves in the far field. There are also

near-field and far-field regimes for the nonlinear regime. One must take the Coriolis force into account in the far field for wave propagation across the wide ocean (TITOV *et al.*, 2003). The advantage of the linear theory is that it allows one to explore the parameter space in earthquake faulting parameters and the spatial dependence of the impinging wave height along the coast on the earthquake faulting parameters.

A typical calculation for a 2000 × 2000 grid point configuration, using the shallow-water linear equations, takes around a few hours on a dual-core 2.3 GHz laptop. The elapsed time of the wave-propagation across a regional extent is about the same as the wall-clock time of the computer simulation.

In properly simulating a run-up process, which is part of the phenomenon that directly impacts society, one would need at least the two-dimensional nonlinear equations and better yet, 3-D nonlinear equations, which is one of the focuses in this paper (shown in Table 1). This is a challenging problem, as it involves very careful implementation of numerical schemes using the actual bottom topography. This procedure is also very expensive computationally and requires massively parallel computing with tens of processors to accomplish 3-D simulations on the order of a few days. We summarize the hierarchy of tsunami simulations in Figure 1, where we classify the ease of computation with the level of mathematical approximations of the tsunami equations of motion. They span from fully 3-D Navier-Stokes equations to the linear two-dimensional shallow-water

Table 1

*Shows the hierarchy of tsunami numerical research in recent years*

| Model | Data Needed | Model Name and Reference |
|---|---|---|
| 1-D equation, Travel time assumption | Topography, Earthquake Magnitude | JRC http://tsunami.jrc.it/ |
| 2-D equations | Topography | INGV |
| Shallow water theory, Finite difference | Fault Parameters, Earthquake Mechanism | http://www.ingv.it/ |
| 2-D Shallow water equations, linear and nonlinear wave propagation, Leap and frog finite-difference schemed | Topography, Fault Parameters, Earthquake Mechanism | TSUNAMI, http://www.tsunami.civil.tohoku.ac.jp/c-indexe.html |
| 2-D Shallow equations, tsunami generation, propagation and inundation modeling; Extended Boussinesq equations | Topography, Fault Parameters, Earthquake Mechanism | MOST http://nctr.pmel.noaa.gov/model.html FUNWAVE, WAVESIM and etc. |
| 2-D/3-D modeling, Finite differences, finite element, finite volume | Topography, Initial Wave Turbulence | Delft3D http://www.wldelft.nl/soft/d3d/intro/index.html |
| 2-D/3-D modeling, Finite elements | Topography Fault Parameters, Earthquake Mechanism | Fastflo http://www.cmis.csiro.au/fastflo/ |
| 2-D/3-D Smoothed Particle Hydrodynamics modeling | Topography | SPH http://www.cmis.csiro.au/cfd/sph/index.html |

equations, with the 2-D nonlinear equations in between. Table 1 shows some of tsunami numerical models developed in recent years. We also try to summarize certain efforts taken including those from one-dimensional empirical equations to full three-dimensional strongly coupled models. Although there are still other important models, and numerical methods are not included in this table, we emphasize here that using the full 3-D Navier-Stokes equations to simulate tsunami hazards needs to be emphasized in future research.

In section 2 we will lay out the shallow-water equations in both linear and nonlinear formats. Next we will discuss the construction of parallel numerical codes used for solving tsunami equations with new techniques from software engineering. In section 4 discuss the preparation of the topography data needed for the numerical simulation. In section 5 we discuss the numerical solution of the 3-D set of tsunami equations. In section 6 we show the results with an emphasis on current visualization techniques. Finally, in section 7 we give a summary and future perspectives.

## 2. *Shallow-Water Equations*

Physical modeling of tsunami wave propagation is a difficult and complex task. A full description and simulation require the use of proper numerical algorithms and corresponding reliable software run on parallel supercomputers (MAJDA 2003; ARBIC *et al*., 2004). This is far too time-consuming and not feasible for most real-time applications of tsunami warning, which needed to be precomputed, however. The simplified theory of tsunami waves that reasonably approximates the realistic behavior of ocean waves over vast open sea is the coupled partial differential equations known as the shallow-water equations (LAYTON and VAN DE PANNE, 2002; PELINOVSKY *et al*., 2001). Basically, this is nonlinear and satisfies not only the far-field but also the near-field tsunami propagation.

The shallow water equations are derived with the fundamental scaling parameter $\delta$, which is relevant to the tsunami wavefield, i.e., water depth over wavelength,

$$\delta = \frac{D}{L} \ll 1. \tag{1}$$

here $D$ is the vertical scale and $L$ is the horizontal scale. With this condition, the 3-D equations can be reduced to 2-D and not pose a fundamental problem for application of the model. As shown by PEDLOSKY (1987), the major deficiency is the absence of density stratification present in the real ocean. Boussinesq approximation is also used where the disturbance of the dimensions is small compared with its mean value. The static fluid pressure assumes that gravity is balanced with the vertical pressure gradient,

$$0 \approx -\frac{1}{\rho}\frac{\partial p}{\partial z} - g \tag{2}$$

and the incompressible assumption,

$$\nabla \cdot \mathbf{v} = 0. \tag{3}$$

With these approximations, the motions of the ocean waves can be expressed in Cartesian coordinates as,

$$\frac{\partial u}{\partial t} + u\frac{\partial u}{\partial x} + v\frac{\partial u}{\partial y} + g\frac{\partial h}{\partial x} - 2\Omega v \sin\phi = 0, \tag{4}$$

$$\frac{\partial v}{\partial t} + u\frac{\partial v}{\partial x} + v\frac{\partial v}{\partial y} + g\frac{\partial h}{\partial y} + 2\Omega u \sin\phi = 0, \tag{5}$$

$$\frac{\partial h}{\partial t} + \frac{\partial}{\partial x}[(h - h_B)u] + \frac{\partial}{\partial y}[(h - h_B)v] = 0. \tag{6}$$

Here, $u$ and $v$ are the horizontal components of water particle velocities $\mathbf{v}$ in the x and y direction, $h$ in the continuity equation is the sum of water depth plus earthquake/landslide vertical displacement, $h_B$ is described as water depth or the sea bottom topography. $\Omega$ is the angular velocity of Earth's rotation and $\phi$ is the latitude. $g$ is the gravitational acceleration.

A more simplified linear theory can be expressed as:

$$\frac{\partial u}{\partial t} + g\frac{\partial h}{\partial x} = 0, \tag{7}$$

$$\frac{\partial v}{\partial t} + g\frac{\partial h}{\partial y} = 0, \tag{8}$$

$$\frac{\partial h}{\partial t} + \frac{\partial}{\partial x}[(h - h_B)u] + \frac{\partial}{\partial y}[(h - h_B)v] = 0. \tag{9}$$

For far-field tsunami wave propagation, linear theory is adequate, but for the near field and the run-up process, shallow water theory with the convection term is needed. The Coriolis force term can also be included to account for the spherical inertial effect.

The viscous stress term of the bottom friction is also included in the very popular TSUNAMI model (IMAMURA *et al.*, 2006). In this case, the equations can be expressed as

$$\frac{\partial u}{\partial t} + u\frac{\partial u}{\partial x} + v\frac{\partial u}{\partial y} + g\frac{\partial h}{\partial x} - 2\Omega v \sin\phi + \frac{1}{2g}\frac{f}{h}u\sqrt{(u^2 + v^2)} = 0, \tag{10}$$

$$\frac{\partial v}{\partial t} + u\frac{\partial v}{\partial x} + v\frac{\partial v}{\partial y} + g\frac{\partial h}{\partial y} + 2\Omega u \sin\phi + \frac{1}{2g}\frac{f}{h}v\sqrt{(u^2 + v^2)} = 0, \tag{11}$$

$$\frac{\partial h}{\partial t} + \frac{\partial}{\partial x}[(h - h_B)u] + \frac{\partial}{\partial y}[(h - h_B)v] = 0, \tag{12}$$

where $f$ is the friction coefficient, which can be spatially dependent. $H = h - h_B$ is the thickness of the fluid layer.

In general, this type of shallow water equation can be solved with the finite-difference method using different schemes, such as upwind total variation diminishing (TVD)

scheme (YEE *et al*., 1983). Multigrid methods may also be utilized to obtain better performance in numerical computing (ADAMS, 2000; BREZINA *et al*., 2004).

Finite-volume methods are becoming increasingly more popular for strongly nonlinear hyperbolic cases, if the convection term dominates over the other terms, especially when the waves break upon arriving at the coast (WEI *et al*., 2006).

In this paper, we propose using a least-squares scheme in the finite-element method to take full advantage of unstructured meshes to portray fractal-like features, in order to represent coastal bathymetry more exactly. This will be discussed in the next section. More importantly, we introduce a novel way to generate FORTRAN source code for finite-element computing that can run on a distributed parallel system. We present this work based on a parallel computing environment which we have developed for many years.

## *3. Parallel Codes for Tsunami Wave Propagation Using Modern Software Engineering*

In geosciences, the major aim is to obtain an accurate physical model to understand the physics correctly. Mathematics forms the basis of this link. For the governing partial differential equations, adding an extra term or changing an existing linear coefficient to include nonlinearity often means difficult and Laborious work for coding. This process is very tedious and is prone to errors.

There has been recent progress in software development, in which parallel finite-element (FEM) codes in FORTRAN language, suitable for massively parallel computing, can be readily generated by modern advances in software engineering. Using this type of approach, we have taken an initiative (ZHANG *et al*., 2005, 2007; SHI *et al*., 2006) in generating codes for a variety of geodynamical problems which include crustal deformation, mantle convection and now tsunami wave propagation.

In this section we demonstrate a modeling language-based parallel finite-element computing environment as the direct link between computational mathematics and geosciences. The FORTRAN source code generated from this system can be run on distributed parallel machines without any modifications. All the environment users need to input to this system are the expressions of PDEs and their corresponding algorithm expressions.

We can show this system and our method of coding as follows. First is the partial differential equations File (shallow.pde file). Figure 2 is an example specifically designed for the nonlinear tsunami equations.

The shallow.pde file is one of the input files in which we use the operator splitting method, in which the calculation process is divided into three steps. We use the Galerkin virtual displacement method, least-squares finite-element and Galerkin virtual displacement method to solve the elliptic terms, convection term and diffusion term, respectively. Although it seems to be complicated numerically, this procedure can handle the strong nonlinear terms associated with tsunami waves, especially for the run-up process. The

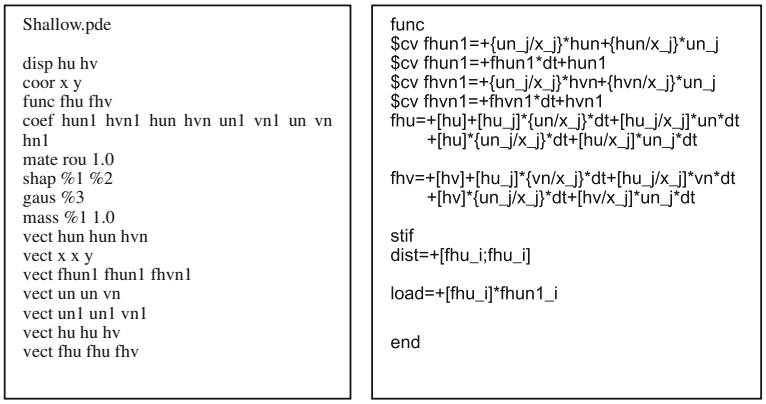

```
Shallow.pde

disp hu hv
coor x y
func fhu fhv
coef hun1 hvn1 hun hvn un1 vn1 un vn
hn1
mate rou 1.0
shap %1 %2
gaus %3
mass %1 1.0
vect hun hun hvn
vect x x y
vect fhun1 fhun1 fhvn1
vect un un vn
vect un1 un1 vn1
vect hu hu hv
vect fhu fhu fhv
```

```
func
$cv fhun1=+{un_j/x_j}*hun+{hun/x_j}*un_j
$cv fhun1=+fhun1*dt+hun1
$cv fhvn1=+{un_j/x_j}*hvn+{hvn/x_j}*un_j
$cv fhvn1=+fhvn1*dt+hvn1
fhu=+[hu]+[hu_j]*{un/x_j}*dt+[hu_j/x_j]*un*dt
      +[hu]*{un_j/x_j}*dt+[hu/x_j]*un_j*dt

fhv=+[hv]+[hu_j]*{vn/x_j}*dt+[hu_j/x_j]*vn*dt
      +[hv]*{un_j/x_j}*dt+[hv/x_j]*un_j*dt

stif
dist=+[fhu_i;fhu_i]

load=+[fhu_i]*fhun1_i


end
```

Figure 2

This is the English-like expressions of the convection terms of shallow water equations. We use vector expression and make the whole finite element weak form very briefly. Hu and hv are the variables (unknowns), hun, hvn, un1, vn1, un, vn, hn1 are all initial values of current time step unknowns. " Fun" section means that we are defining new functions. The "stiff" and "load" sections are the expressions for the stiffness matrix and right-hand side, respectively.

algorithm expression based on the computing environment can be written simply in the Generalized Coupling Nonlinear file (shallow.gcn), as shown in Figure 3.

When all files have been input to this computing environment, this system will automatically generate FORTRAN program segments from the information of partial differential equations and algorithm expressions, as shown in Figure 4.

These program segments will then be inserted into a common program stencil, to different locations respectively, as shown in Figure 5. In this manner the entire source code package is generated. This software package, which is based on a distributed parallel computing architecture machine and message passing interface (MPI) system (www.mpi-forum.org), together with parallel solvers for large-scale linear systems and

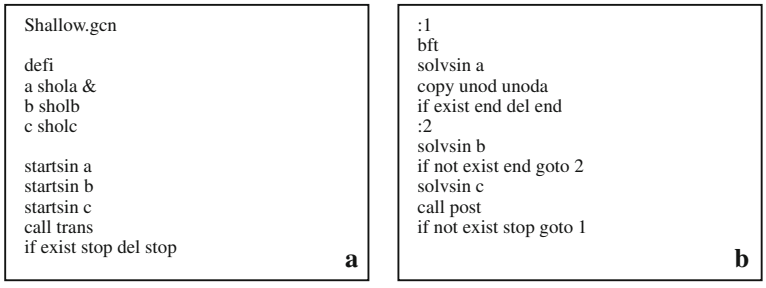

```
Shallow.gcn

defi
a shola &
b sholb
c sholc

startsin a
startsin b
startsin c
call trans
if exist stop del stop
```

**a**

```
:1
bft
solvsin a
copy unod unoda
if exist end del end
:2
solvsin b
if not exist end goto 2
solvsin c
call post
if not exist stop goto 1
```

**b**

Figure 3

(a) and (b) are the first and second parts of one GCN file. This file resembles a scripts file to communicate to the computing environment for generating various source codes, using different program stencils. Another scripts file will also be generated according to this input file, which can run all the programs generated after the compilation.

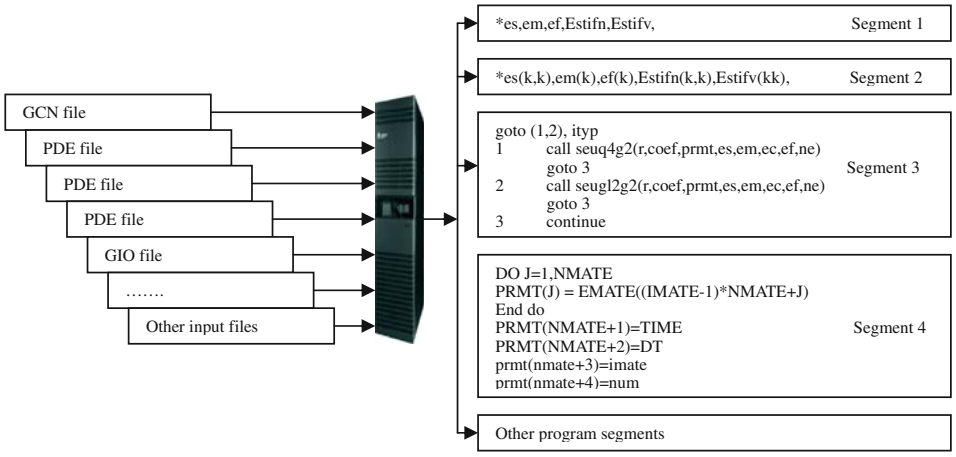


Figure 4

This schematic diagram illustrates how this computing environment generates all the source code according to the input files. The GIO file will describe the format of preprocessing files, such as the different element types, element factors, coordination system, initial values and constrained boundary information. The PRMT part of the generated program segment is derived basically from the GIO file.

automatic mesh and data partition system, can be compiled and run in parallel without any changes. Users can download the source code from the generation server via the client software interface. This is a typical prototype of the grid-computing environment. We will continue work on this area.

In this case, all the algorithmic expressions are already stored in the system library and can be used directly. A typical algorithm expression for elliptic type of partial differential equation is expressed as shown in Figure 5. More details of the modeling language and the computational environment can be seen in our recent paper (ZHANG *et al*., 2007).

## *4. Three-Dimensional Tsunami Modeling*

Besides epidemic control and post-tsunami recovery, a timely and effective warning system is one of the most crucial elements to determine the threat to the coastal communities. This warning system can consist of gathering as much information as possible on the potential tsunamis, estimation of their frequency, detecting the dynamic process of fault rupturing and sea-floor deformations along the main thrusts of plate boundaries, tsunami formation, tsunami wave propagation and the coastal region inundated. Technical issues of tsunami modeling and forecasting, tsunami formation, tsunami wave propagation and run-up process are still the persistent research problems. Wave propagation over short distances (near field) and long distances (far field) are quite different because of Coriolis acceleration and the friction effects of sea-bed sediment

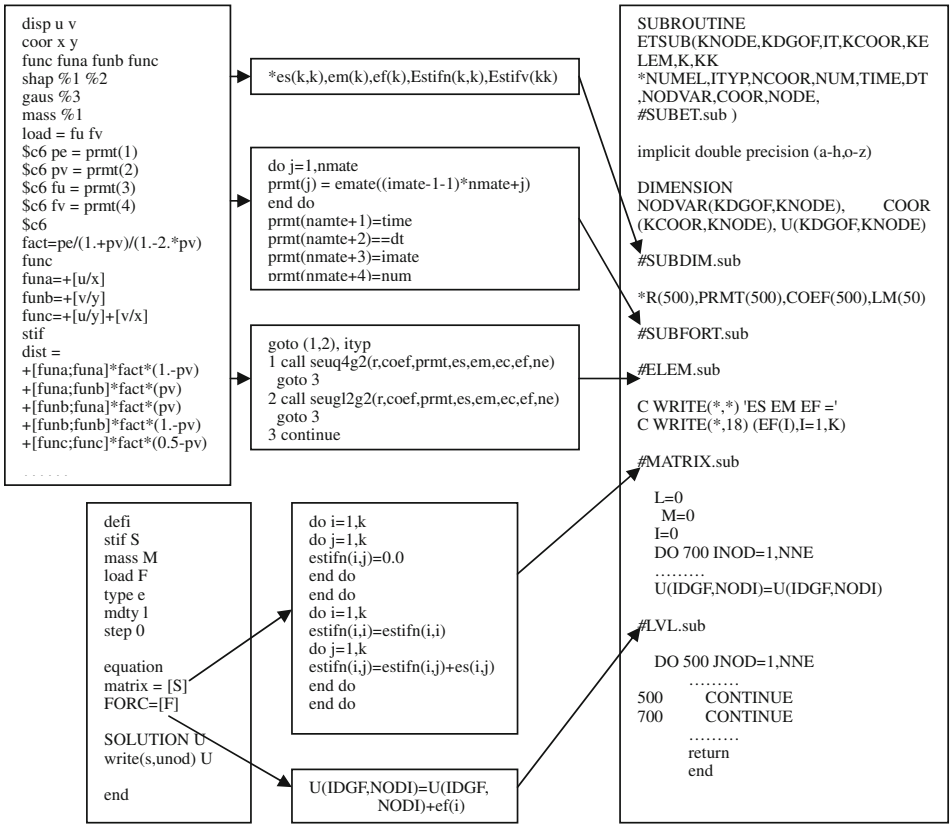


Figure 5

Generation of FORTRAN source codes which are solved by the FEM (finite-element) method. The left two columns show the input finite-element modeling language, the upper part is the expressions of partial differential equations, and the lower part shows the solving algorithmic expressions of the elliptic type PDEs. The modeling language-based computing environment will generate program segments (center column) according to these expressions, then all the program segments will be inserted into a program stencil for assembling as a FORTRAN-77 styled source code (the very right column).

layer. For the run-up processes, the shallow water equations are not feasible to model the highly nonlinear hyperbolic phenomena.

The construction of the initial water depth distribution is of vital importance for a full three-dimensional simulation of tsunami propagation. We have used the GTOP30 data for continental topography and SRTM30 data for bathymetry (sea-floor topography) to generate the finite-element mesh describing the sea-floor profile and landscape around them. This makes it feasible to obtain the water depth distribution within this area by means of generating water meshes over the bathymetry profile and local mesh refinement in the costal areas. We use unstructured mesh generation technology to produce the finite-element mesh grid describing the actual water body. Figure 6 shows this process of generating the highly irregular finite-element meshes.

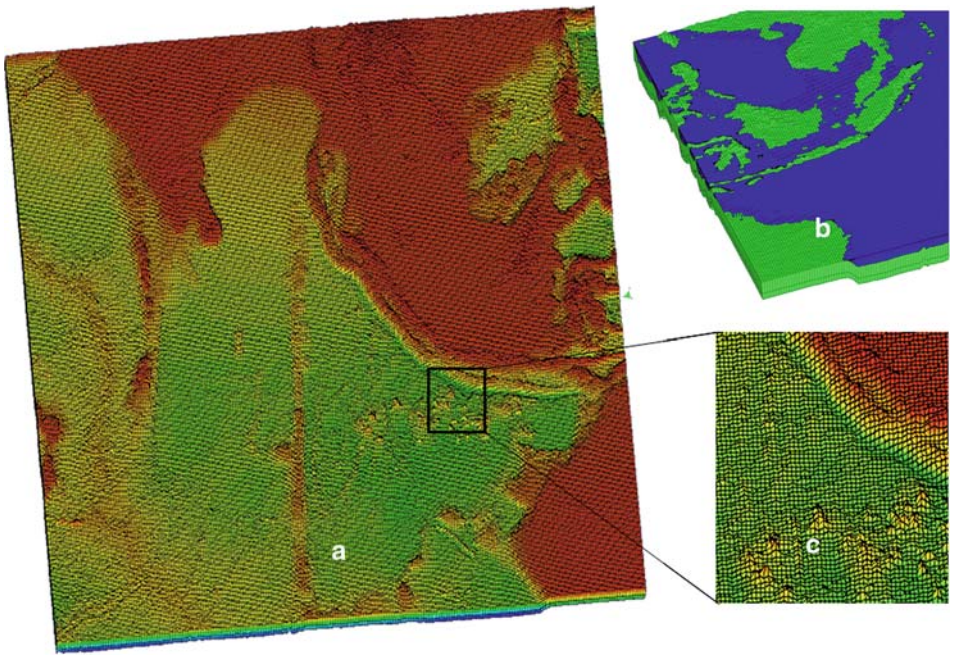


Figure 6
These three graphs show how we generate the finite-element mesh of sea-bed and sea-water layer distribution and make it consistent with the profile of sea-floor data. (a) shows the topography data from GTOP 30, (b) shows how to generate the finite-element mesh of the seawater over sea-floor bathymetry, (c) shows the zoomed-in section of one portion of the whole area. Because the upper layer of this water body is more important than the lower layer, we have used special mesh size distribution to refine the mesh on the top part of the sea-water layer.

The topography of the sea-bed can be regarded as a basin of seawater, thus we just delete the mesh elements of sea-bed and all water layer mesh elements whose thicknesses are less that 0.01 meter. These thin mesh elements will cause numerical singularities during the numerical simulation. Figure 7 shows the result of water body distribution and the finite-element mesh.

Sediment layer effect (or bottom friction effect) contributes greatly to tsunami wave propagation over long distance. The shallow water equations always have this mechanism as a friction term. In realistic three-dimensional model construction, we also need such data. In this case, we use the lowest layer of seawater as the mixture of sediment and seawater and assign different material factors, such as a higher rheological coefficient (Minoura *et al*., 2005).

With the help of high performance computing infrastructure, it is also possible for us to take coupling process of sea-floor seismic wave propagation and tsunami wave propagation into consideration (Cacchione *et al*., 2002; Gower, 2005; Lui *et al*., 2005). We show this kind of nonlinear coupling and the associated finite-element mesh generated as shown in Figure 8.

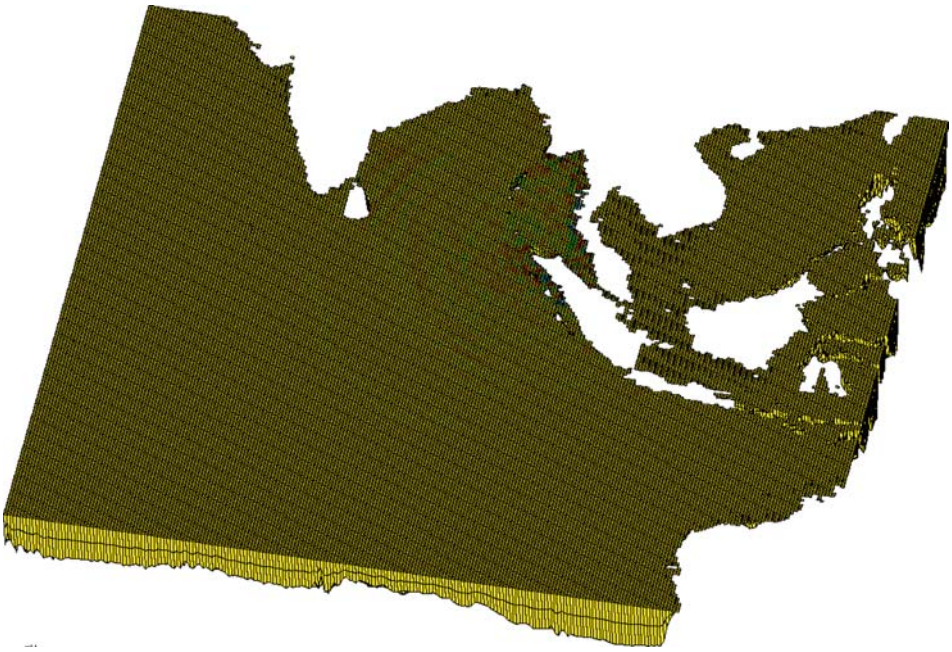

Figure 7
Water distribution and the finite-element mesh.

We developed both sequential and parallel versions of tsunami propagation. The sequential version of the 3-D finite-element model has more than 180,000 mesh nodes and the parallel 3-D version has more than 2 million finite-element nodes. We ran the parallel version on a 32-node PC cluster. The total run time was about 6 hours. In the next section we will show the simulation results from this type of modeling.

## *5. Numerical Solution of the Set of 3-D Tsunami Equations*

Using automatic grid generation methods, we have devised a finite-element based code, for the three stages which culminates with the use of the augmented Lagrangian method (DANILOV *et al.*, 2004; FORTIN and GLOWINSKI, 1983; ARǴAEZ and TAPIA, 2002; BERTSEKAS, 1996) for the run-up process, as well as the Arbitrary Lagrange-Euler Configuration method (LONGATTE *et al.*, 2003) to address the free surface problem near shore. Our continuous efforts are focused on seeking novel algorithms and state-of-art techniques, in order to unravel the mysteries associated with tsunami wave propagation and wind-driven waves in 3-D. We have cast the Navier-Stokes equations within the framework of an incompressible model with an equation of state for the seawater. Our formulation allows the tracking and simulation of three principal stages, to the formation,

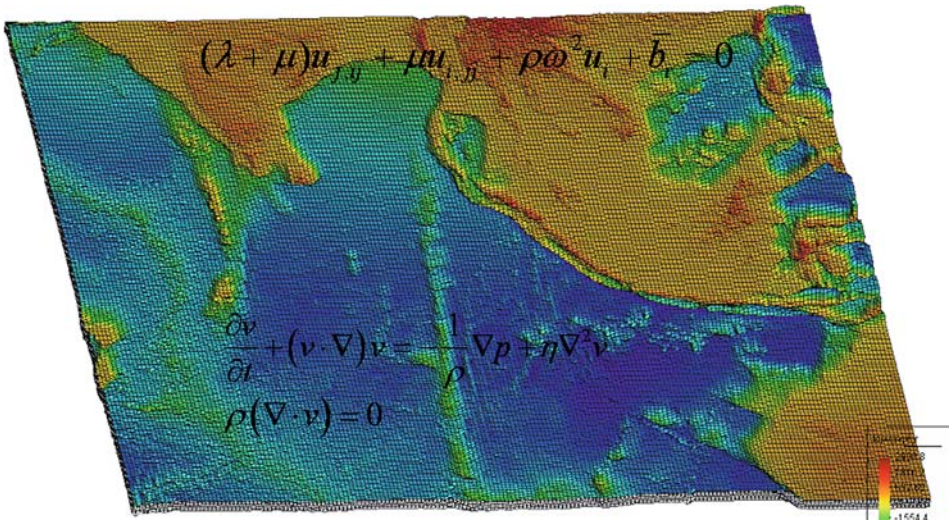


Figure 8
Finite-element mesh for coupled modeling of sea-floor seismic wave propagation and tsunami wave propagation, where and are the displacement and velocity vectors, respectively, and are the Lame elastic constants, is mass density, is circular frequency, and is the body force.

propagation and run-up stages of tsunami and waves coming ashore. These equations are written as the following:

$$\frac{\partial \mathrm{v}}{\partial t}+(\mathrm{v}\cdot\nabla)\mathrm{v}+2\Omega\times\mathrm{v}=-\frac{1}{\rho}\nabla p+f(h(x,y),\gamma(x,y))\mu\nabla^2\mathrm{v}+\kappa p+g, \tag{13}$$

where $\boldsymbol{v}$, $\Omega$ , $p$ and $\eta$ are the velocity, rotation angular velocity, the dynamical pressure and rheology respectively, and $g$ is the gravity acceleration.

$$f=f(h(x,y),\gamma(x,y)) \tag{14}$$

is the factor of relationship between velocity and wavelength with the depth of water distribution, the seabed condition of sediment layer thickness which will absorb energy from tsunami waves while they are propagating. $h(x,y)$ is the parameterized coefficient of velocity and wavelength relationship. $\gamma(x,y)$ is referred to as the impact of sediment layer on the tsunami wave, in dissipating the wave energy.

The relationship of velocity and wavelength with depth of water distribution is shown as Figure 9.

We also need to explain kappa term; this term contains more numerical than physical meaning:

$$\kappa=k(\Delta t,\Delta h) \tag{15}$$

is the augmented Lagrangian multiplier for the pressure term to make it more elliptical-like and stable numerically, when a first-order explicit method is deployed to update the time-dependent equations.

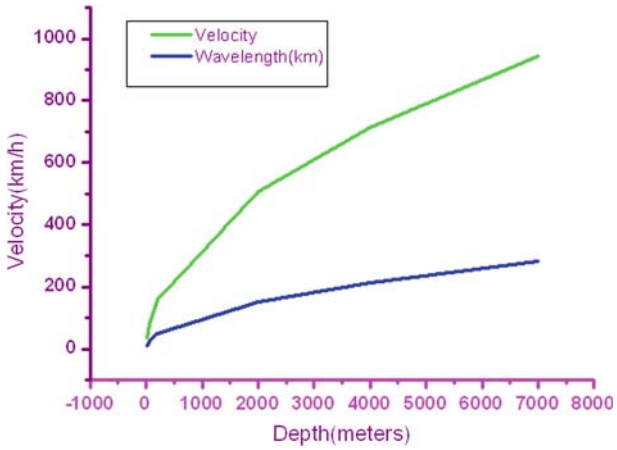


Figure 9
shows the relationship of velocity and wavelength with depth of water distribution. Basically, the velocity of idealized traveling waves on the ocean is wavelength-dependent and for shallow enough depths it also depends upon the depth of the water. This can be formulated as, here is tsunami wavelength, is the water depth (http://hyperphysics.phy-astr.gsu.edu/hbase/watwav.html#c3).

The operator-splitting algorithm (BRUSDAL *et al.*, 1998; MARINOVA *et al.*, 2003) is utilized to solve these Navier-Stokes (NS) equations. This numerical computing scheme uses different methods to solve different types of partial differential equations, respectively. All these equations are from the same NS equation set. We use this algorithm mainly because this kind of algorithm can allow the strong nonlinear processes of run-up processes while the tsunami reaches the seashore, which may lead to an unstable numerical solution of finite element and is very difficult to converge. In brief, we describe our algorithm as the following.

Firstly, we solve the diffusion equations, together with the incompressible condition equation,

$$\begin{cases} \dfrac{\partial \mathrm{v}}{\partial t} + 2\Omega \times \mathrm{v} = -\dfrac{1}{\rho}\nabla p + f(h(x,y),\gamma(x,y))\mu\nabla^2 \mathrm{v} + \kappa p + g \\ \nabla \cdot \mathrm{v} = 0 \end{cases} \tag{16}$$

the weak form of these equations is given in terms of inner-products and is written as

$$\begin{cases} \left(\dfrac{\partial \mathrm{v}}{\partial t}, \bar{\mathrm{v}}\right)_\Omega + (2\Omega \times \mathrm{v}, \bar{\mathrm{v}})_\Omega + \left(\dfrac{1}{\rho}\nabla p, \bar{\mathrm{v}}\right)_\Omega - f(h(x,y),\gamma(x,y))\mu(\nabla \mathrm{v}, \nabla \bar{\mathrm{v}})_\Omega = (g, \bar{\mathrm{v}})_\Omega \\ (\nabla \cdot \mathrm{v}, \bar{p})_\Omega - k(p, \bar{p})_\Omega = 0 \end{cases} \tag{17}$$

where

$$k = c \cdot \det. \tag{18}$$

Here $c$ is an independent constant, det is the determinant of element Jacobian matrix.

Then we solve the convection-like equation in the mass-conservation balance,

$$\rho \frac{\partial \mathbf{v}}{\partial t} + \rho(\mathbf{v} \cdot \nabla)\mathbf{v} = 0, \tag{19}$$

using a first-order Euler backward difference scheme

$$\frac{\partial \mathbf{v}}{\partial t} = \frac{\mathbf{v}^{n+1} - \mathbf{v}^n}{dt} \tag{20}$$

and the Newton-Raphson method to linearize this nonlinear term,

$$(\mathbf{v} \cdot \nabla)\mathbf{v} = (\mathbf{v}^n \cdot \nabla)\mathbf{v}^n + (\mathbf{v}^n \cdot \nabla)(\mathbf{v} - \mathbf{v}^n) + ((\mathbf{v} - \mathbf{v}^n) \cdot \nabla)\mathbf{v}^n \tag{21}$$

from equation (22, 23 and 24) we get,

$$\rho \frac{\mathbf{v}^{n+1} - \mathbf{v}^n}{dt} + \rho(\mathbf{v}^n \cdot \nabla)\mathbf{v}^{n+1} + \rho(\mathbf{v}^{n+1} \cdot \nabla)\mathbf{v}^n = \rho(\mathbf{v}^n \cdot \nabla)\mathbf{v}^n \tag{22}$$

another form is

$$\rho\mathbf{v}^{n+1} + dt\rho(\mathbf{v}^n \cdot \nabla)\mathbf{v}^{n+1} + dt\rho(\mathbf{v}^{n+1} \cdot \nabla)\mathbf{v}^n = \rho\mathbf{v}^n + dt\rho(\mathbf{v}^n \cdot \nabla)\mathbf{v}^n. \tag{23}$$

We use the least-squares method (Bochev and Gunzburger, 1993), which is robust for solving hyperbolic equations, to solve this equation,

$$\begin{aligned}
&\rho(L(v_x), L(\bar{v}_x))_\Omega + \rho(L(v_y), L(\bar{v}_y))_\Omega + \rho(L(v_z), L(\bar{v}_z))_\Omega \\
&\quad = \left(\rho\left(v_x^n + dt\left(v_x^n \frac{\partial}{\partial x} v_x^n + v_y^n \frac{\partial}{\partial y} v_x^n + v_z^n \frac{\partial}{\partial z} v_x^n\right)\right), L(\bar{v}_x)\right)_\Omega \\
&\qquad + \left(\rho\left(v_y^n + dt\left(v_x^n \frac{\partial}{\partial x} v_y^n + v_y^n \frac{\partial}{\partial y} v_y^n + v_z^n \frac{\partial}{\partial z} v_y^n\right)\right), L(\bar{v}_y)\right)_\Omega \\
&\qquad + \left(\rho\left(v_z^n + dt\left(v_x^n \frac{\partial}{\partial x} v_z^n + v_y^n \frac{\partial}{\partial y} v_z^n + v_z^n \frac{\partial}{\partial z} v_z^n\right)\right), L(\bar{v}_z)\right)_\Omega
\end{aligned} \tag{24}$$

where $L$ is given by,

$$\begin{aligned}
L(v_x) &= v_x^{n+1} + dt\left(v_x^n \frac{\partial}{\partial x} v_x^{n+1} + v_y^n \frac{\partial}{\partial y} v_x^{n+1} + v_z^n \frac{\partial}{\partial y} v_x^{n+1}\right) \\
&\quad + dt\left(v_x^{n+1} \frac{\partial}{\partial x} v_x^n + v_y^{n+1} \frac{\partial}{\partial y} v_x^n + v_z^{n+1} \frac{\partial}{\partial y} v_x^n\right)
\end{aligned} \tag{25}$$

$$L(v_y) = v_y^{n+1} + dt\left(v_y^n \frac{\partial}{\partial x} v_y^{n+1} + v_x^n \frac{\partial}{\partial y} v_y^{n+1} + v_z^n \frac{\partial}{\partial y} v_y^{n+1}\right) + dt\left(v_y^{n+1} \frac{\partial}{\partial x} v_y^n + v_x^{n+1} \frac{\partial}{\partial y} v_y^n + v_z^{n+1} \frac{\partial}{\partial y} v_y^n\right) \tag{26}$$

$$L(v_z) = v_z^{n+1} + dt\left(v_z^n \frac{\partial}{\partial x} v_z^{n+1} + v_x^n \frac{\partial}{\partial y} v_z^{n+1} + v_y^n \frac{\partial}{\partial y} v_z^{n+1}\right) + dt\left(v_z^{n+1} \frac{\partial}{\partial x} v_z^n + v_x^{n+1} \frac{\partial}{\partial y} v_z^n + v_y^{n+1} \frac{\partial}{\partial y} v_z^n\right) \tag{27}$$

Here we use $v_x$,$v_y$,$v_z$ as the three orthogonal components of **v** for a clear description, and $\bar{v}_x, \bar{v}_y, \bar{v}_z$ is the virtual displacement of $v_x$,$v_y$,$v_z$, respectively. Our developed parallel computing environment is used to generate all the Fortran source code.

Our formulation allows the tracking and simulation of three stages, principally the formation, propagation and the run-up stages of tsunami, culminating with the waves coming ashore. This formulation also allows for the wave surface to be self-consistently determined within a linearized framework and is computationally very fast. The sequential version of this code can run on a workstation with 4 Gbytes memory less than 2 minutes per time step for one million grid points. This code has also been parallelized with MPI-2 and has good scaling properties, nearly linear speedup, which has been tested on a 32-node PC cluster. We have employed the actual ocean sea-floor topographical data to construct oceanic volume and attempt to construct the coastline as realistically as possible, using 11 levels of structure meshes in the radial direction of the Earth. Our initial focus is on the East Coast of Asia. In order to understand the intricate dynamics of the wave interactions, we have implemented a visualization overlay based on the Amira package (http://www.amiravis.com/), a powerful 3-D volume rendering visualization tools for massive data post-processing. The ability to visualize large data sets remotely is also an important objective we are aiming for, as international collaboration is one of the top aims of this research. This part will be displayed in section 7.

## 6. Visualization

The dynamics of tsunami wave propagation are very rich and offer great opportunities for visual studies. Yet the visualization of tsunami wave propagation has not maintained its progress with the advances in visualization being made in mantle convection and earthquake dynamics. A review of the current status of visualization in the geosciences has been given in the COHEN Report (2005). We have employed an interactive system for advanced 3-D visualization and volume rendering, the package Amira (http://www.amiravis.com). This software takes advantage of modern graphics hardware and is available for all standard operating systems, ranging from Linux to MacOS and Windows. The extensive set of easy-to-use features includes data imaging on the Cartesian and

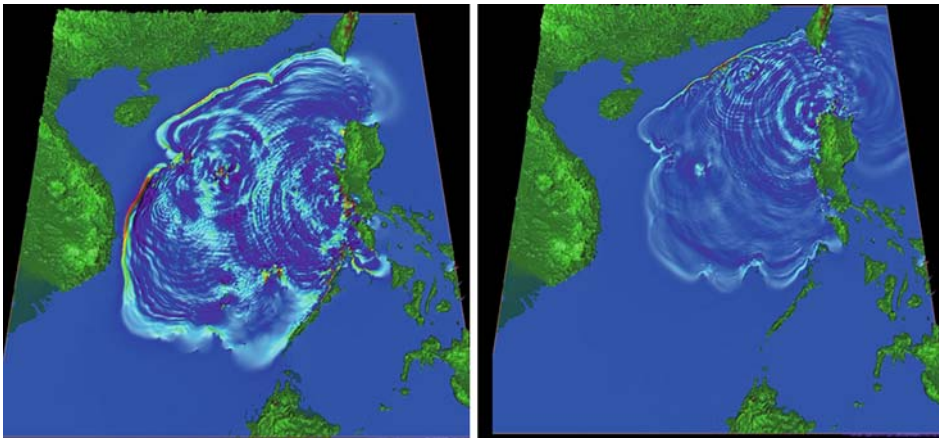

Figure 10
Visualization of tsunami wave propagation in the South China Sea at different time steps, which span less than one hour of real time.

finite-element grids, scalar and vector field visualization algorithms, computation of iso-surfaces, direct volume rendering, time-series manipulation and creating movies, support for the Tcl scripting language and remote data-processing.

Figure 10 shows rendered results computed by the Amira package. The propagation of the tsunami wave over time is clearly demonstrated through the visualization.

The dynamics of tsunami wave-propagation simulation result we are visualizing are always associated with specific geographical regions globally. In the visualization package such as Amira we mentioned above, it is possible to render neighboring terrains together with the simulation visualization. However, for such packages, the semantic geographical information, which is critical for hazard evaluation based on the tsunami wave propagation we simulated, is missing. In our research we start to integrate the visualization result of our simulation with the newly available software Google Earth [Google Earth] for contextual geological information for such visualizations (Fig. 11).

Google Earth is a server-client based virtual globe program (http://earth.google.com/). It maps the entire earth by pasting images obtained from satellite imagery, aerial photography and GIS over a 3-D globe. Many regions are available with at least 15 meters of resolution. Google Earth allows users to search for addresses, enter coordinates, or simply use the mouse to browse to a location. Google Earth also has digital terrain model data collected by NASA's Shuttle Radar Topography Mission. Users can directly view the geological features in three-dimensional perspective projection, instead of as 2-D maps. We use the image overlay function provided by the Google Earth software to integrate our visualization results into a virtual globe context. Image overlay function allows us to map rendered pictures of our visualization result on to the virtual globe with the geographical locations specified by the user. The transparency of the


Figure 11
Visualization of tsunami simulation results using Google Earth software with Power-Wall Display (http://www.lcse.umn.edu).

mapped pictures can be tuned to between 0 (totally transparent) and 1 (totally opaque). In Figure 11, one time frame of tsunami wave propagation simulation results is mapped to the Google Earth and projected to a multi-panel PowerWall display to allow careful, close inspections. Note in the figure, that the cities and other important geographical locations under the impact of the simulated tsunami simulation are clearly visible to the viewer. Such a tool could greatly, enhance the interpolation and presentation of our tsunami wave-propagation simulation results.

The seismic displacement itself is multi-scale in nature. Although the earthquake extends its deformation throughout the whole far field, only regions in the near field have large displacement.

The Google Earth enables the users to navigate the whole virtual globe with integrated visualizations at different level of details. As illustrated in Figure 12, the user can freely zoom to different levels of resolution to either obtain a global view or a close look. Note that in the most zoomed-out image, Google Earth provides the recorded earthquake information indicated by a red dot in the studied region. Such information is valuable for researchers seeking to understand the event. The visualization results we embed in Google Earth could also be saved in a data exchange format (KML) together with the geological context information. Such data could be directly opened by other parties who have the software.

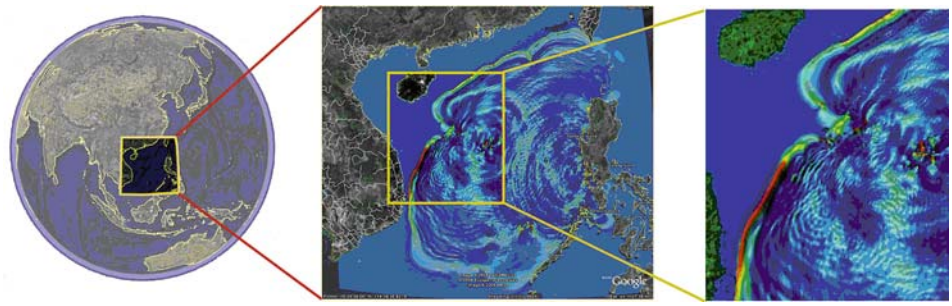

Figure 12
Visualization of tsunami simulation results in the South China Sea at multi-level of details.

## 7. Conclusions and Perspectives

We have laid out the hierarchy of the different levels of partial differential equations needed to solve the tsunami problem, ranging from the linear shallow-water equation to the fully nonlinear 3-D Navier-Stokes equations in which the role of sedimentary layer is introduced as a regularizing agent for stabilizing the numerical solution near the shore. We regard that the forecasting and tsunami-warning problem may be best attacked with the linear shallow-water equation, because of the enormous computational efforts needed for solving the nonlinear shallow water equations and the full 3-D equations. We cannot over stress the importance of using the physics of sedimentary processes in stabilizing the most vicious nonlinearities during the run-up stage in the 3-D problem.

We have described the visualization of both the seismic displacements and tsunami wave propagation using the Amira visualization package and our own developed method using the graphics processing unit (GPU), which offers a low-cost solution from which to solve a graphically intensive task such as the construction of InSAR images. We have also presented a technique for overlaying our calculations atop the map using Google Earth. This innovation will assist the reader to better understand the multi-scale physical phenomena associated with tsunami waves.

## Acknowledgement

This work is supported by the National Science Foundation of China under Grant Numbers 40474038, 40374038 and by the National Basic Research Program of China under Grant Number 2004cb418406 and and U.S. National Science Foundation under the ITR and EAR programs. This work was conducted as part of the visualization working group at the laboratory of computational geodynamics supported by the Graduate University of Chinese Academy of Sciences. We thank Shi Chen and Shaolin Chen as members of the visualization working group who provided some of the figures. We thank Mark S. Wang for technical assistance.

## References


Adams, M.F. (2000), *Algebraic multigrid methods for constrained linear systems with applications to contact problems in solid mechanics*, Numerical Linear Algebra with Applications *11*(2–3), 141–153.

Amira, http://www.amiravis.com.

Arbic, B.K., Garner, S.T., Hallberg, R.W., and Simmons, H.L. (2004), *The accuracy of surface elevations in forward global barotropic and baroclinic tide models*, Deep-Sea Res. *II* 51, 3069–3101.

Argaez, M., and Tapia, R.A. (2002), *On the global convergence of a modified augmented Lagrangian line search interior-point method for Nonlinear Programming*, J. Optimiz. Theory Applicat. *114*, 1–25.

ARSC, http://www.arsc.edu/challenges/2005/globaltsunami.html.

Asian Tsunami Videos, http://www.asiantsunamivideos.com/.

Barnes, W.L., Pagano, T.S., and Salomonson, V.V. (1998), *Prelaunch characteristics of the Moderate Resolution Imaging Spectroradiometer (MODIS) on EOS-AM1*, IEEE Trans. Geosci. Remote Sensing *36*, 1088–1100.

Bertsekas, D.P., *Constrained Optimization and Lagrange Multiplier Methods* (Athena Scientific, Belmont 1996).

Bochev, P. and Gunzburger, M. (1993), *A least-squares finite-element method for the Navier-Stokes equations*, Appl. Math. Lett. *6*, 27–30.

Brezina, M., Falgout, R., MacLachlan, S., Manteuffel, T., McCormick, S., Ruge, J. (2004), *Adaptive smoothed aggregation*, SIAM J. Sci. Comp. *25*, 1896–1920.

Brusdal, K., Dahle, H.K., Karlsen, K.H., and Mannseth, T. (1998), *A study of the modelling error in two operator splitting algorithms for porous media flow*, Comput. Geosci. *2*(1), 23–36.

Butler, D. (2006), *Virtual globes: The web-wide world*, Nature *439*, 776–778.

Cacchione, D.A., Pratson, L.F., and Ogston, A.S. (2002), *The shaping of continental slopes by internal tides*, Science *296*, 724–727.

Chang, C., and Gunzburger, M. (1990), *A subdomain Galerkin/least-squares method for first order elliptic systems in the plane*, SIAM J. Numer. Anal. *27*, 1197–1211.

Chang, H.C., Ge, L., and Rizos, C. (2005), *Asian Tsunami Damage Assessment with Radarsat-1 SAR Imagery*, http://www.gmat.unsw.edu.au/snap/publications/chang_etal2005e.pdf.

Chen, Q., Kirby, J. T., Dalrymple, R. A., Kennedy, A. B., and Chawla, A., 2000, *Boussinesq modeling of wave transformation, breaking and runup. II: Two horizontal dimensions*, J. Waterway, Port, Coastal and Ocean Engin. *126*, 48–56.

Cohen, R.E. (2005), *High-Performance Computing Requirements for the Computational Solid Earth Sciences*, http://www.geo-prose.com/computational_SES.html.

Danilov, S., Kivman, G., and Schroeter, J. (2004), *A finite-element ocean model: Principles and evaluation*, Ocean Modelling *6*, 125–150.

Fortin, M. and Glowinski, R., *Augmented Lagrangian Methods: Applications to the Numerical Solution of Boundary-Value Problems* (Elsevier Science, New York, 1983).

Geist, E.L., Titov, V.V., and Synolakis, C.E. (2006), *Tsunami: Wave of change*, Scientific American, *294*(1), 56–63.

Gica, E. and Teng, M.H., *Numerical modeling of earthquake generated distant tsunamis in the Pacific Basin*, Proc 16 ASCE Engin. Mech. Conf., (University of Washington, Seattle 2003).

Gill, A.E., *Atmosphere-Ocean Dynamics* (Academic Press, New York 1982).

Gonzalez, F.I., Satake, K., Boss, E.F., and Mofjeld, H.O. (1995), *Edge wave and non-trapped modes of the 25 April 1992 Cape Mendocino tsunami*, Pure Appl. Geophys. *144*(3/4), 409–426.

Google Earth, http://earth.google.com/.

Gower, J. (2005), *Jason 1 detects the 26 December 2004 tsunami*, EOS Transact. Am. Geophy. Union *86*(4), 37–38.

Gower, J. (2005), *Jason 1 detects the 26 December 2004 tsunami*, EOS Transact. Am. Geophys. Union, *86*(4), 7–38.

Guo, J.Y., *Fundamental Geophysics* (Surveying and Mapping Press, China, 2001).

*Hyperphysics*, http://hyperphysics.phy-astr.gsu.edu/hbase/watwav.html#c3.

Imamura, F. *et al.* (2006), Tsunami Modeling Manual.

ISPRS, http://www.isprs.org/istanbul2004/.

JRC, http://tsunami.jrc.it/model/model.asp.

KEES, C.E. and MILLER, C.T. (2002), *Higher order time integration methods for two-phase flow*, Adv. Water Resources *25*, 159–177.

KENNEDY, A.B, CHEN, Q., KIRBY, J.T., and DALRYMPLE, R.A. (2000), *Boussinesq modeling of wave transformation, breaking and runup. I: One dimension*, J. Waterway, Port, Coastal and Ocean Engin. *126*, 39–47.

KENNEDY, A.B. and KIRBY, J.T. (2003), *An unsteady wave driver for narrow-banded waves: Modeling nearshore circulation driven by wave groups*, Coastal Engin. *48*(4), 257–275.

KIRBY, J. T. and DALRYMPLE, R. A. (1986), *Modelling waves in surfzones and around islands*, J. Waterway, Port, Coastal and Ocean Engin. *112*, 78–93.

LAYTON, A.T., and VAN DE PANNE, M. (2002), *A numerically efficient and stable algorithm for animating water waves*, Visual Comput. *18*, 41–53.

LONGATTE, E., BENDJEDDOU, Z., and SOULI, M. (2003), *Application of arbitrary Lagrange-Euler formulations to flow-induced vibration problems*, J. Pressure Vessel Technol. *125*(4), 411–417.

LUI, P. L.F., LYNETT, P., FERNANDO, H., JAFFE, B.E., HIGMAN, B., MORTON, R., GOFF, J., and SYNOLAKIS, C. (2005), *Observations by the international tsunami survey team in Sri Lanka*, Science, *308*, 1595.

MAJDA, A.J. (2003), *Introduction to PDEs and waves for the atmosphere and ocean*, Courant Lecture Notes 9, Am. Math. Soc.

MARINOVA, R.S., CHRISTOV, C.I., and MARINOV, T.T. (2003), *A fully coupled solver for incompressible Navier-Stokes equations using operator splitting*, Internat. J. Comp. Fluid Dyn. *17*(5), 371–385.

MEINIG, C., STALIN, S.E., NAKAMURA, A.I., GONZALEZ, F., and MILBURN, H.G. (2005), *Technology developments in real-time tsunami measuring, monitoring and forecasting in oceans*, MTS/IEEE, 19–23 September 2005, Washington, D.C.

MINOURA, K., IMAMURA, F., KURAN, U., NAKAMURA, T., PAPADOPOULOS, G.A., SUGAWARA, D., TAKAHASHI, T., YALCINER, A.C. (2005), *A tsunami generated by a possible submarine slide: Evidence for slope failure triggered by the North Anatolian fault movement*, Natural Hazards *36–3*(10), 297–306.

MOBAHERI, M.R. and MOUSAVI, H. (2004), *Remote sensing of suspended sediments in surface waters using MODIS images*, Proc. XXth ISPRS Congress, Geo-Imagery Bridging Continent, Istanbul, 12 –23.

MOFJELD, H.O., TITOV, V.V., GONZALEZ, F.I., and NEWMAN J.C. (2000), *Analytic theory of tsunami wave scattering in the open ocean with application to the North Pacific Ocean*, NOAA Tech. Memor. ERL PMEL-116, 38.

MPI, www.mpi-forum.org.

NAEIJE, M.E., DOORNBOS, L., *et al.* (2002), *Radar altimeter database system: Exploitation and Extension (RADSxx)*, Final Report, NUSP-2 Report 02–06.

NOURBAKHSH, I., SARGENT, R., WRIGHT, A., CRAMER, K., MCCLENDON, B., and JONES, M. (2006), *Mapping disaster zones*, Nature *439*, 787–788.

ORMAN, J.V., COCHRAN, J.R., WEISSEL, J.K., and JESTIN, F. (1995), *Distribution of shortening between the Indian and Australian plates in the central Indian Ocean*, Earth Planet. Sci. Lett. *133*, 35–46.

PEDLOSKY, J., *Geophysial Fluid Dynamics* (Springer-Verlag, New York 1987).

PELINOVSKY, E., TALIPOVA, T., KURKIN, A., and KHARIF, C. (2001), *Nonlinear Mechanism of Tsunami Wave Generation by Atmospheric Disturbances*, Natural Hazard and Earth Sci. *1*, 243–250.

SHI, Y.L., ZHANG, H., LIU, M., YUEN, D., and WU, Z.L. (2006), *Developing a viable computational environment for geodynamics*, WPGM, Beijing, (Abstract).

SMITH, W.H.F., SCHARROO, R., TITOV, V.V., ARCAS, D., and ARBIC, B.K. (2005), *Satellite altimeters measure tsunami*, Oceanography *18*(2), 10–12.

SWANSON, R.C. (1992), *On central-difference and upwind schemes*, J. Comp. Phys. *101*, 292–306.

TANG, L., CHAMBERLIN, C. *et al.* (2006), *Assessment of potential tsunami impact for Pearl Harbor, Hawaii*. NOAA Tech. Memo. OAR PMEL.

TIBBETTS, J. (2002), *Coastal Cities: Living on the Edge. In Environmental Health Perspectives*, 110(11), http://ehp.niehs.nih.gov/members/2002/110–11/focus.html.

TITOV, V.V. and GONZALEZ, F.I. (1997), *Implementation and testing of the Method of Splitting Tsunami (MOST) model*, NOAA Tech. Memo. ERL PMEL-112, 11.

TITOV, V.V., GONZALEZ, F.I., BERNARD, E.N., EBLE, M.C., MOFJELD, H.O., NEWMAN, J.C., and VENTURATO, A.J. (2005), *Real-time tsunami forecasting: Challenges and solutions*, Natural Hazards *35*(1), 41–58.

TITOV, V.V., GONZALEZ, F.I., MOFJELD, H.O., and VENTURATO, A.J. (2003), *NOAA time seattle tsunami mapping project: procedures, data sources, and products*, NOAA Tech. Memo. OAR PMEL-124.

TITOV, V.V., MOFJELD, H.O., GONZALEZ, F.I., and NEWMAN J.C. (1999), *Offshore forecasting of Alaska-Aleutian Subduction Zone tsunamis in Hawaii*, NOAA Tech. Memo. ERL PMEL-114, 22.

TITOV, V.V., RABINOVICH, A.B. *et al*. (2005), *The global reach of the 26 December 2004 Sumatra Tsunami*, Science, DOI: 10.1126/science, 1114576.

UNEP-WCMC IMAPS, http://nene.unep-wcmc.org/imaps/tsunami/viewer.htm.

VAN WACHEM, B.G.M., and SCHOUTEN, J.C. (2002), *Experimental validation of 3-D Lagrangian VOF model: Bubble shape and rise velocity*, AIChE J. *48*(12), 2744–2753.

WALKLEY, M. and BERZINS, M. (2002) *A finite-element method for the two-dimensional extended Boussinesq equations*, Internat. J. Num. Meth. in Fluids *39*(10), 865–885, 2002.

WEI, Y., MAO, X.Z., and CHEUNG, K.F. (2006), *Well-balanced finite-volume model for long-wave runup*, J. Waterway, Port, Coastal and Ocean Engin. *132*(2), 114–124.

YEE, H.C., WARMING, R.F., and HARTEN, A. (1983), *Implicit total variation diminishing (TVD) schemes for steady-state calculations*, Comp. Fluid Dyn. Conf. *6*, 110–127.

ZHANG, H., SHI, Y.L., LIU, M., WU, Z.L., and LI, Q.S. (2005), *A China-US collaborative effort to build a web-based grid computational environment for geodynamics*, Am. Geophys. Union, Fall (Abstract).

ZHANG HUAI, LIU MIAN, SHI YAOLIN, DAVID A. YUEN, YAN ZHENZHEN, and LIANG GUOPING, *Toward an automated parallel computing environment for geosciences*, Phy. Earth Planet. Inter., in press, accepted manuscript, available online 24 May 2007.

(Received October 31, 2006, revised August 1, 2007, Accepted August 6, 2007)
Published Online First: April 2, 2008